

Luminescent Gold(I) and Silver(I) Complexes of 2-(Diphenylphosphino)-1-methylimidazole (dpim): Characterization of a Three-Coordinate Au(I)–Ag(I) Dimer with a Short Metal–Metal Separation

Vincent J. Catalano* and Stephen J. Horner

Department of Chemistry, University of Nevada at Reno, Reno, Nevada 89557

Received June 20, 2003

The Au(I) and Ag(I) closed-shell metal dimers of 2-(diphenylphosphino)-1-methylimidazole, dpim, were investigated. dpim formed the discrete binuclear species $[\text{Ag}_2(\text{dpim})_2(\text{CH}_3\text{CN})_2]^{2+}$ (**1**) when reacted with appropriate Ag(I) salts. Likewise, $[\text{Au}_2(\text{dpim})_2]^{2+}$ (**3**) and $[\text{AuAg}(\text{dpim})_3]^{2+}$ (**4**) were produced via reactions with (tht)AuCl, tht is tetrahydrothiophene, and Ag(I). Compound **3** exhibits an intense blue luminescence ($\lambda_{\text{max}} = 483 \text{ nm}$) in the solid state. However, upon initial formation of **3**, a small impurity of Cl^- was present giving rise to an orange emission ($\lambda_{\text{max}} = 548 \text{ nm}$). Attempts to form $[\text{Au}_2(\text{dpim})_2]\text{Cl}_2$ yielded only (dpim)AuCl (**2**), which is not visibly emissive. The rare three-coordinate heterobimetallic complex $[\text{AuAg}(\text{dpim})_3]^{2+}$ (**4**) exhibits intense luminescence in the solid-state resembling that of **3**. The crystal structures of **1–4** were determined, revealing strong intramolecular aurophilic and argentophilic interactions in the dimeric compounds. Compound **1** has an Ag(I)–Ag(I) separation of 2.9932(9) Å, while compound **3** has a Au(I)–Au(I) separation of 2.8174(10) Å. Compound **4** represents the first example of a three-coordinate Au(I)–Ag(I) dimer and has a metal–metal separation of 2.8635(15) Å. The linear Au(I) monomer, **2**, has no intermolecular Au(I)–Au(I) interactions, with the closest separation greater than 6.8 Å.

Introduction

It is well-known that coordination compounds of gold(I) often aggregate with Au(I)–Au(I) separations shorter than the sum of their van der Waals radii.^{1–4} These interactions have been termed aurophilic.⁵ The closed-shell (d^{10} – d^{10}) interactions of monovalent gold have been widely documented both experimentally and theoretically for a variety of mono- and multinuclear Au(I) compounds.^{6,7} While intermolecular aurophilic interactions commonly form polymeric systems,^{1,6} the formation of discrete Au–Au dimers is often utilized to facilitate our understanding of the forces involved in aurophilic bonding.^{7,8} Because gold(I) has a known affinity for phosphorus, and to a lesser extent nitrogen,^{4–8} numerous diphosphine and phosphine–imine

mixed-donor ligands have been employed as bridging ligands to hold two Au(I) ions in close proximity.

Bis(diphenylphosphino)methane (dppm) and bis(dicyclohexylphosphino)methane (dcpm) are representative of the diphosphine ligands, while diphenylphosphinopyridine (dppy), dimethylphosphinopyridine (dmpp), and 2-(diphenylphosphino)-1-benzylimidazole (BzImPh₂P) are representative of the mixed-donor species commonly used to prepare Au(I) dimers.^{9–12} Even though the dppm and dcpm ligands are very flexible and capable of separations of 2.4–3.6 Å,¹³ the $[(\text{dppm})_2\text{Au}_2]^{2+}$ and $[(\text{dcpm})_2\text{Au}_2]^{2+}$ complexes contain Au–

* To whom correspondence should be addressed. E-mail: vjc@unr.edu.

- (1) Schmidbaur, H. *Nature* **2001**, *413*, 31–33.
- (2) Gade, L. H. *Angew. Chem., Int. Ed.* **2001**, *40*, 3573–3575.
- (3) Fernández, E. J.; Laguna, A.; López-de-Luzuriaga, J. M. *Gold Bull.* **2001**, *34*, 14–19.
- (4) Yam, V. W.-W.; Lo, K. K.-W. *Chem. Soc. Rev.* **1999**, *28*, 323–334.
- (5) Scharbaum, F.; Grohmann, A.; Huber, B.; Krüger, C.; Schmidbaur, H. *Angew. Chem., Int. Ed. Engl.* **1988**, *27*, 1544–1546.
- (6) Puddephatt, R. J. *Coord. Chem. Rev.* **2001**, *216–217*, 313–332.
- (7) (a) Pykkö, P.; Zhao, Y. *Angew. Chem., Int. Ed. Engl.* **1991**, *30*, 604–605. (b) Pykkö, P. *Chem. Rev.* **1997**, *97*, 597–636.

- (8) (a) Crespo, O.; Fernández, E. J.; Jones, P. G.; Laguna, A.; López-de-Luzuriaga, J. M.; Mendía, A.; Monge, M.; Olmos, E. *J. Chem. Soc., Chem. Commun.* **1998**, 2233–2234. (b) Wang, S.; Garzón, G.; King, C.; Wang, J.-C.; Fackler, J. P., Jr. *Inorg. Chem.* **1989**, *28*, 4623–4629. (c) Wang, S.; Fackler, J. P., Jr.; King, C.; Wang, J. C. *J. Am. Chem. Soc.* **1988**, *110*, 3308–3310.
- (9) (a) Fu, W.-F.; Chan, K.-C.; Miskowski, V.-M.; Che, C.-M. *Angew. Chem., Int. Ed.* **1999**, *38*, 2783–2785. (b) Leung, K. H.; Phillips, D. L.; Mao, Z.; Che, C.-M.; Miskowski, V. M.; Chan, C.-K. *Inorg. Chem.* **2002**, *41*, 2054–2059. (c) Leung, K. H.; Phillips, D. L.; Tse, M.-C.; Che, C.-M.; Miskowski, V. M. *J. Am. Chem. Soc.* **1999**, *121*, 4799–4803.
- (10) Olmos, M. E.; Schier, A.; Schmidbaur, H. *Z. Naturforsch. B* **1997**, *52*, 203–208.
- (11) King, C.; Wang, J.-C.; Khan, M. N. I.; Fackler, J. P., Jr. *Inorg. Chem.* **1989**, *28*, 2145–2149.

Au separations of 2.8–3.1 Å.⁹ The more rigid dmpp ligand constrains the metal–metal separation, and [dmpp₂Au₂](BF₄)₂ has a Au–Au separation of only 2.776 Å.¹⁴ More recently, silver(I) complexes of similar ligands have been shown to exhibit argentophilic bonding analogous to the Au(I) systems.¹⁵ Pyykkö and Laguna¹⁶ recently reported theoretical studies suggesting that systems containing heterometallic Au–Ag interactions will have even shorter metal–metal separations than their homometallic analogues. The occurrence of Au(I)–Ag(I) dinuclear complexes is limited, and they are of current interest.¹⁵

One important property of the Au(I)–Au(I) complexes is that they are often intensely luminescent,^{2–4,17} making them attractive with respect to possible application toward luminescent display devices¹⁸ and luminescent sensors.¹⁹ The emission maxima of the dinuclear complexes is red-shifted compared to their mononuclear analogues.¹¹ The origin of the emission from Au(I) dimers was previously thought to be associated with the metal-localized $5d\sigma^* \rightarrow 6p\sigma$ transition.⁹ However, in a recent series of papers, Che and co-workers argue that the visible emission is actually associated with an exciplex formation where Au–L, Au–solvent, and Au–counterion interactions play a significant role.⁹ Che demonstrated that the emission of [(dcpm)₂Au₂]²⁺ depends on the coordinating ability of the counterion, with the

emission maxima of 368 nm for the ClO₄[−] salt and 530 nm for the I[−] complex in the solid state.^{9a}

Previously we have utilized larger mixed-donor phosphine ligands to form metallocryptands²⁰ that include three-coordinate Au(I) species, which are also known to be luminescent.²¹ The gold–metallocryptands are capable of encapsulating other closed-shell metal ions to induce Au–M interactions, where M = Tl(I) or Hg(0), within the cages.²⁰ These mixed-metal systems are highly luminescent²⁰ and provide a method by which compounds may be altered to produce a wide range of emissive complexes. In an effort to create more simple systems containing Au–M interactions, the use of other mixed-donor ligands capable of bridging must be considered. We report here a study including a mononuclear Au(I) and the dinuclear Au(I)–Au(I), Ag(I)–Ag(I), and Au(I)–Ag(I) complexes of 2-(diphenylphosphino)-1-methylimidazole (dpim).

Results

dpim was synthesized according to a literature procedure.²² Complexes **1–4** were synthesized in acetonitrile solution at room temperature. All of the complexes reported here are air-stable and with the exception of **3** soluble in common organic solvents including acetonitrile, dichloromethane, and acetone.

According to Scheme 1, the dimeric silver(I) complex [Ag₂(dpim)₂(CH₃CN)₂](ClO₄)₂, **1**, was prepared by reacting 1 equiv of Ag(ClO₄)·H₂O with 1 equiv of dpim. Removal of solvent and trituration of the residue with diethyl ether afforded the colorless, microcrystalline solid. The monomeric gold(I) complex (dpim)AuCl, **2**, was formed by reacting 1 equiv of (tht)AuCl, where tht = tetrahydrothiophene, with 1 equiv of dpim. The solvent volume was reduced over mild heat, and the complex crystallized upon cooling to room temperature. The dimeric gold(I) complexes [Au₂(dpim)₂](ClO₄)₂·2CH₃CN, **3**(ClO₄), and [Au₂(dpim)₂](BF₄)₂·2CH₃CN, **3**(BF₄), were prepared by reacting 1 equiv of (tht)AuCl with 1 equiv of Ag(ClO₄)·H₂O or AgBF₄ respectively. After removal of the AgCl precipitate, the complexes were crystallized from the reaction mixtures via slow diffusion of diethyl ether at −5 °C. In a preparation similar to **3**, the heterobimetallic complex [AuAg(dpim)₃](ClO₄)₂, **4**, was formed by reacting 1 equiv of (tht)AuCl with 2 equiv of Ag(ClO₄)·H₂O and 3 equiv of dpim. After removal of AgCl precipitate, the filtrate was evaporated to dryness. The residue was triturated with diethyl ether to give **4** as a colorless, microcrystalline solid.

The most striking feature of **3** is its solid-state luminescence. As seen in Figure 1, crystalline complexes of **3** exhibit two distinctly different emission spectra with different excitation modes. Upon *initial* formation of **3**, the crystals exhibit a visibly orange luminescence ($\lambda_{\text{max}} = 548 \text{ nm}$, $\lambda_{\text{ex}} = 336 \text{ nm}$) when excited with a hand-held UV lamp. However, upon crushing, heating, or recrystallization the complex luminesces blue ($\lambda_{\text{max}} = 483 \text{ nm}$, $\lambda_{\text{ex}} = 368 \text{ nm}$).

- (12) (a) Burini, A.; Pietroni, B. R.; Galassi, R.; Valle, G.; Calogero, S. *Inorg. Chim. Acta* **1995**, *229*, 299–305. (b) Bachechi, F.; Burini, A.; Fontani, M.; Galassi, R.; Macchioni, A.; Pietroni, B. R.; Zanello, P.; Zuccaccia, C. *Inorg. Chim. Acta* **2001**, *323*, 45–54. (c) Tejel, C.; Bravi, R.; Ciriano, M. A.; Oro, L. A.; Bordonaba, M.; Graiff, C.; Tiripicchio, A.; Burini, A. *Organometallics* **2000**, *19*, 3115–311. (d) Burini, A.; Galassi, R.; Pietroni, B. R.; Rifaiani, G. *J. Organomet. Chem.* **1996**, *519*, 161–167.
- (13) (a) Zhang, H.-X.; Che, C.-M. *Chem.–Eur. J.* **2001**, *7*, 4887–4893. (b) Li, Z.; Loh, Z.-H.; Mok, K. F.; Hor, T. S. A. *Inorg. Chem.* **2000**, *39*, 5299–5305. (c) Balch, A. L.; Catalano, V. J. *Inorg. Chem.* **1992**, *31*, 3934–3942.
- (14) Inoguchi, Y.; Milewski-Mahrla, B.; Schmidbaur, H. *Chem. Ber.* **1982**, *115*, 3085–3095.
- (15) Rawashdeh-Omary, M. A.; Omary, M. A.; Fackler, J. P., Jr. *Inorg. Chim. Acta* **2002**, *334*, 376–384.
- (16) Fernández, E. J.; Laguna, A.; López-de-Luzuriaga, J. M.; Monge, M.; Pyykkö, P.; Runeberg, N. *Eur. J. Inorg. Chem.* **2002**, 750–753.
- (17) Forward, J. M.; Fackler, J. P., Jr.; Assefa, Z. In *Optoelectronic Properties of Inorganic Compounds*; Roundhill, D. M., Fackler, J. P., Jr., Eds.; Plenum Press: New York, 1999; p 195.
- (18) Ma, Y.; Che, C.-M.; Chao, H.-Y.; Zhou, X.; Chan, W.-H.; Shen, J. *Adv. Mater.* **1999**, *11*, 852–857.
- (19) Mansour, M. A.; Connick, W. B.; Lachicotte, R. J.; Gysling, H. J.; Eisenberg, R. *J. Am. Chem. Soc.* **1998**, *120*, 1329–1330.
- (20) (a) Catalano, V. J.; Kar, H. M.; Bennett, B. L. *Inorg. Chem.* **2000**, *39*, 121–127. (b) Catalano, V. J.; Bennett, B. L.; Noll, B. C. *J. Chem. Soc., Chem. Commun.* **2000**, 1413–1414. (c) Catalano, V. J.; Bennett, B. L.; Yson, R.; Noll, B. C. *J. Am. Chem. Soc.* **2000**, *121*, 10056–10062. (d) Catalano, V. J.; Bennett, B. L.; Kar, H. M.; Noll, B. C. *J. Am. Chem. Soc.* **1999**, *121*, 10235–10236. (e) Catalano, V. J.; Malwitz, M. A.; Noll, B. C. *J. Chem. Soc., Chem. Commun.* **2001**, 581–582.
- (21) (a) Crespo, O.; Gimeno, M. C.; Jones, P. G.; Laguna, A.; López-de-Luzuriaga, J. M.; Monge, M.; Pérez, J. L.; Ramón, M. A. *Inorg. Chem.* **2003**, *42*, 2061–2068. (b) McCleskey, T. M.; Gray, H. B. *Inorg. Chem.* **1992**, *31*, 1733–1734. (c) Che, C.-M.; Yip, H.-K.; Yam, V. W.-W.; Cheung, P.-Y.; Lai, T. F.; Shieh, S.-J.; Peng, S.-M. *J. Chem. Soc., Dalton Trans.* **1992**, 427–433. (d) King, C.; Khan, M. N. I.; Staples, R. J.; Fackler, J. P., Jr. *Inorg. Chem.* **1992**, *31*, 3236–3238. (e) Khan, M. N. I.; Staples, R. J.; King, C.; Fackler, J. P., Jr.; Wippeny, R. E. *Inorg. Chem.* **1993**, *32*, 5800–5807. (f) Shie, S. J.; Li, D.; Peng, S.-M.; Che, C.-M. *J. Chem. Soc., Dalton Trans.* **1993**, 195–196. (g) Yam, V. W.-W.; Lee, W.-K. *J. Chem. Soc., Dalton Trans.* **1993**, 2097–2100. (h) Forward, J. M.; Assefa, Z.; Fackler, J. P., Jr. *J. Am. Chem. Soc.* **1995**, *117*, 9103–9104.

- (22) Jalil, M. A.; Yamada, T.; Fujinami, S.; Honjo, T.; Nishikawa, H. *Polyhedron* **2001**, *20*, 627–633.

Scheme 1

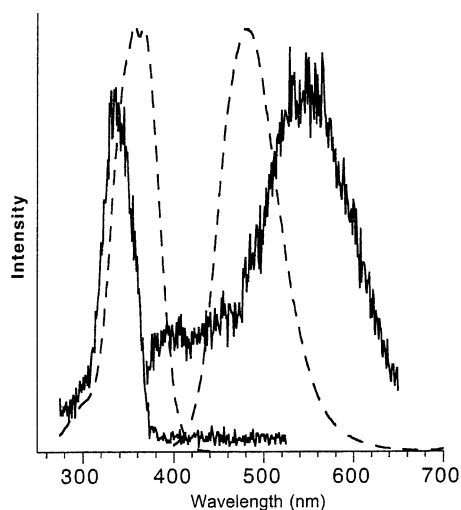
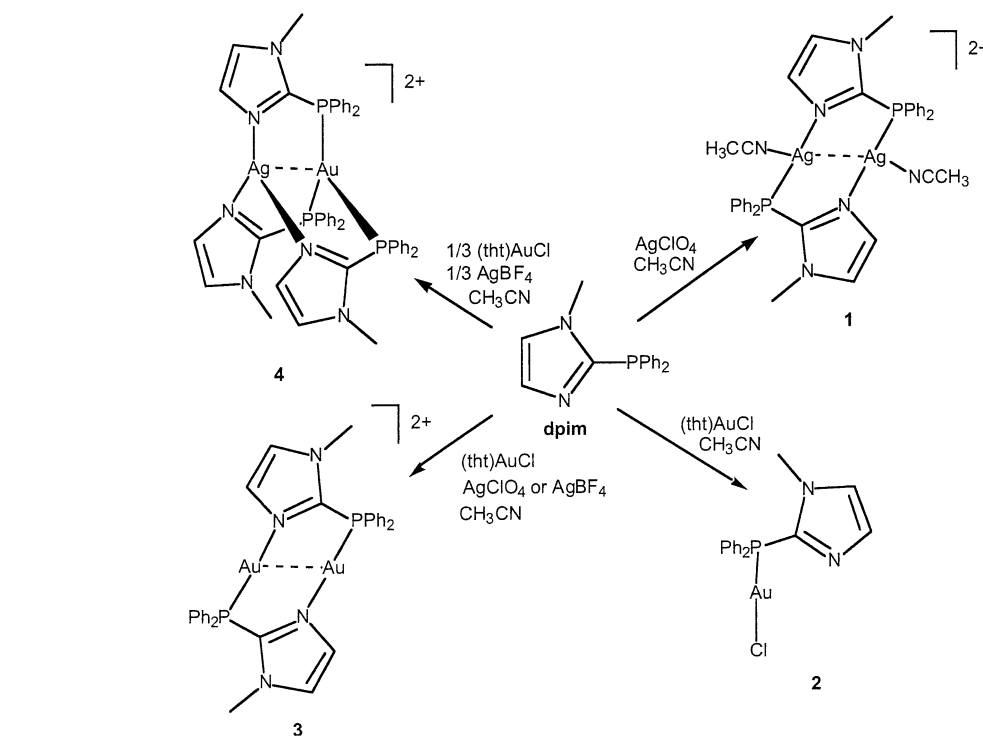


Figure 1. Normalized solid-state excitation (left) and emission (right) spectra of **3**-orange (solid) and **3**-blue (dashed), at room temperature.

The emission intensity of the “blue” crystals is much higher than that of the “orange” crystals, while the luminescence from “blue” powder is significantly more intense to the eye than the “blue” crystals. Upon crushing or heating, the intense blue emission swamps the weaker orange signal making it appear (incorrectly) that this mechanical action has converted the orange form into the blue form. Once “orange” **3** is purified by recrystallization to form the “blue” form, the “orange” form becomes inaccessible. Thus far, the “orange” form can only be reproduced by repeating the initial synthesis. The formation of the two species with vastly different colored emissions is independent of solvents of crystallization, as both forms have been prepared from acetonitrile, propionitrile, benzonitrile, and even 1,2-dichloroethane. Changing from perchlorate to tetrafluoroborate anions

appears to have no effect upon the emission. The metrical parameters from the crystal structures of **3**(ClO₄) or **3**(BF₄), regardless of emission color, are identical (vide infra). This, coupled with the ability to reproduce the formation of both the “orange” and “blue” under various reaction conditions, suggests that the origin of the contrasting emissions may be an impurity from the initial synthesis of **3** (vide infra) and is likely related to incomplete halide abstraction by Ag⁺ ion.

Unlike **3**, the emission spectra of crystals of **1**, **2**, and **4** are much less complicated. The emission spectrum of **1** consists of a broad, featureless band at 442 nm (λ_{ex} 355 nm) that tails out to 600 nm. Complexes **2** and **4** also exhibit broad, featureless emission bands that tail out beyond 600 nm. However, the emission maxima are at 493 nm (λ_{ex} = 335 nm) and 490 nm (λ_{ex} = 360 nm) respectively, and the excitation spectra are not identical. The emission and excitation spectra of crystalline **4** are presented in Figure 2. Visibly, **1** and **2** luminesce blue-white, while **4** is yellow, when illuminated with a hand-held lamp (λ_{ex} = 366 nm).

In solution the emission maxima are significantly blue-shifted. Complexes **1** and **4** display a single, featureless emission band at room temperature at 370 nm (λ_{ex} = 294 nm) and 354 nm (λ_{ex} = 290 nm), respectively. The emission spectra of **2** and **3** consist of broad emission bands in the UV region that extend beyond 550 nm. Complex **2** emits at 376 nm with a secondary band at 443 nm (λ_{ex} = 294 nm). Complexes **3**(ClO₄) and **3**(BF₄) emit at 360 nm with a secondary band at 431 nm (λ_{ex} = 290 nm). These emission spectra are similar to that of free dpim ligand under similar conditions. An acetonitrile solution of dpim emits at 360 and 493 nm (λ_{ex} = 296 nm); however, the lower energy band dominates the spectrum. A concentration dependence study of the emission for **3** in acetonitrile shows that as the

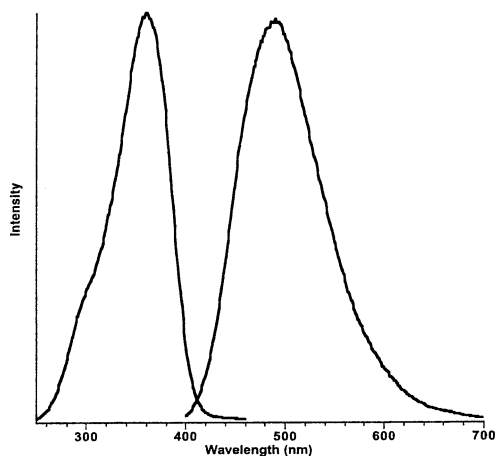


Figure 2. Solid-state excitation (left) and emission (right) spectra of $[\text{AuAg}(\text{dpim})_3](\text{ClO}_4)_2$, **4**.

concentration increases (from 10^{-6} to 10^{-4} M incrementally) the intensity of the high energy emission band at 360 nm is decreased. At the same time a low-energy (431 nm) band appears and increases in intensity while red-shifting to 493 nm. There is also a dramatic decrease in the overall intensity of emission as the concentration is increased suggesting an intermolecular process at higher concentrations.

The electronic absorption spectra of **1–4** in acetonitrile solution are nearly identical to that of the free dpim. dpim exhibits strong $\pi-\pi^*$ bands at 233 and 252 nm. Complexes **1–4** exhibit intense absorptions in the ranges of 230–232 nm and 248–252 nm.

The $^{31}\text{P}\{^1\text{H}\}$ NMR spectroscopy is consistent with the formulations presented in Scheme 1. The spectra of **2–4** are comprised of sharp single resonances at 12.1, 18.9, and 17.5 ppm, respectively, with no evidence of ^{107}Ag or ^{109}Ag coupling in **4**. All attempts to determine the extent of Cl^- ion contamination in the initial preparation of **3** by NMR spectroscopy were thwarted by low solubility in acetonitrile and the complete lack of solubility in chloroform. This resulted in spectra with no definition from the baseline of any resonance except that associated with **3**. The $^{31}\text{P}\{^1\text{H}\}$ NMR spectrum of **1** consists of a broad multiplet at -4.9 ppm, arising from the complicated coupling to ^{107}Ag ($I = 1/2$, 51.8% abundance) and ^{109}Ag ($I = 1/2$, 48.2% abundance).

Crystals of **1** suitable for X-ray diffraction analysis were grown by slow diffusion of diethyl ether into a saturated acetonitrile solution of the complex at room temperature. A thermal ellipsoid plot of **1** is presented in Figure 3 with selected bond distances and angles presented in Table 1. The colorless complex crystallizes in the monoclinic space group $P2_1/c$ with an inversion center midway between the silver atoms, making only half of the complex crystallographically unique. The asymmetric unit also contain one ClO_4^- anion, one acetonitrile molecule bound the silver, and one and one-half acetonitrile solvates. The two silver atoms are bridged by two dpim ligands in a head to tail fashion. Each silver is three coordinate, bound to a phosphorus atom of one ligand, an imine nitrogen of the second ligand, and to an acetonitrile molecule. The $\text{N}(2\text{a})-\text{Ag}(1)-\text{P}(1)$, $\text{N}(2\text{a})-\text{Ag}(1)-\text{N}(3)$, and

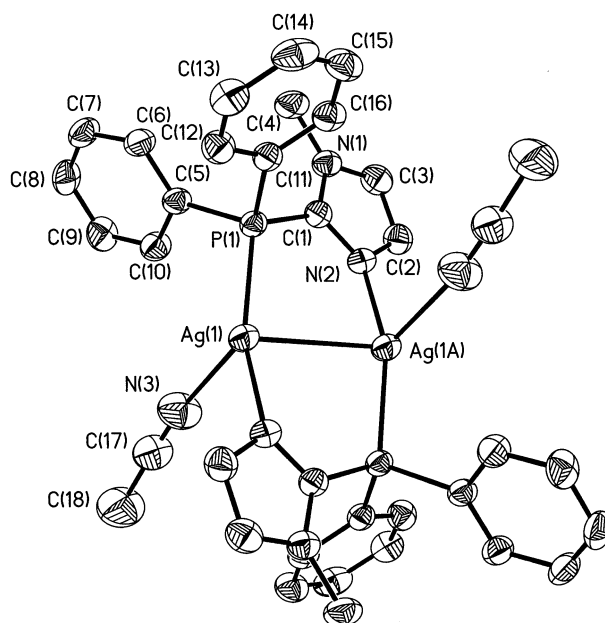


Figure 3. Thermal ellipsoid plot (40%) of the cationic portion of **1**. Only the crystallographically unique portion and Au(1A) are numbered. Hydrogen atoms are removed for clarity.

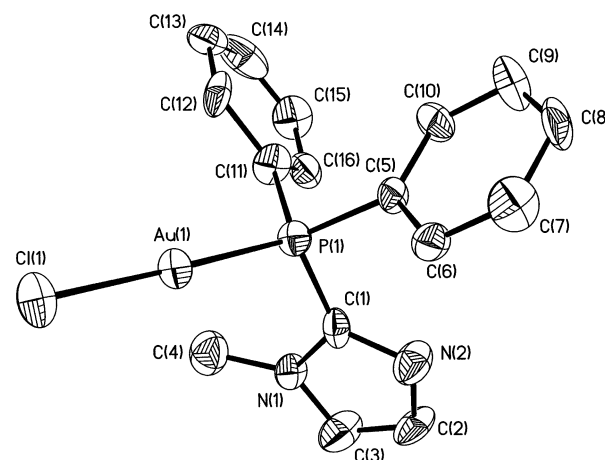


Figure 4. X-ray structural drawing of complex **2**. Thermal ellipsoids are drawn at 40%.

Table 1. Selected Bond Lengths (Å) and Angles (deg) for **1**

$\text{Ag}(1)\cdots\text{Ag}(1\text{A})$	2.9932(9)	$\text{P}(1)-\text{C}(1)$	1.809(6)
$\text{Ag}(1)-\text{P}(1)$	2.3807(14)	$\text{P}(1)-\text{C}(5)$	1.831(5)
$\text{Ag}(1)-\text{N}(2\text{A})$	2.198(4)	$\text{P}(1)-\text{C}(11)$	1.814(6)
$\text{Ag}(1)-\text{N}(3)$	2.506(6)		
$\text{P}(1)-\text{Ag}(1)-\text{N}(2\text{A})$	157.54(12)	$\text{P}(1)-\text{Ag}(1)-\text{Ag}(1\text{A})$	83.94(4)
$\text{P}(1)-\text{Ag}(1)-\text{N}(3)$	115.38(16)	$\text{N}(3)-\text{Ag}(1)-\text{Ag}(1\text{A})$	104.53(17)
$\text{N}(3)-\text{Ag}(1)-\text{N}(2\text{A})$	86.75(19)	$\text{C}(1)-\text{P}(1)-\text{C}(11)$	406.4(2)
$\text{N}(2\text{A})-\text{Ag}(1)-\text{Ag}(1\text{A})$	86.62(12)		

$\text{P}(1)-\text{Ag}(1)-\text{N}(3)$ angles are 157.54(12), 86.75(19), and 115.38(16) $^\circ$ respectively. The Ag–Ag separation is 2.9932(9) Å.

X-ray-quality crystals of **2** form upon cooling a warm, saturated acetonitrile solution of **2** to 0 $^\circ\text{C}$. Figure 4 shows a thermal ellipsoid drawing of **2** with selected bond distances and angles presented in Table 2. The colorless complex crystallizes in the orthorhombic space group $P2_12_12_1$. The two-coordinate Au(I) atoms are nearly linear with the angle $\text{P}(1)-\text{Au}(1)-\text{Cl}(1)$ of 178.8(2) $^\circ$ and $\text{Au}(1)-\text{P}(1)$ and Au-

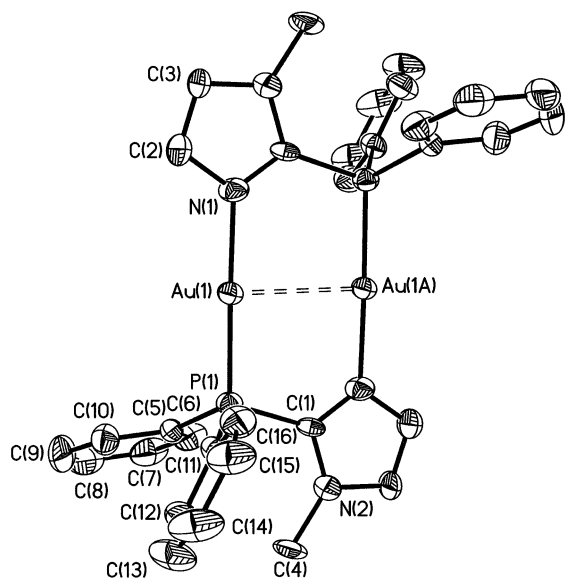


Figure 5. Thermal ellipsoid plot (40%) of the cationic portion of $3(\text{ClO}_4)_2$. Only the crystallographically unique portion and Au(1A) are labeled. Hydrogen atoms removed for clarity.

Table 2. Bond Lengths (Å) and Angles (deg) for **2**

Au(1)–P(1)	2.227(6)	P(1)–C(1)	1.80(2)
Au(1)–Cl(1)	2.293(7)	P(1)–C(5)	1.803(19)
P(1)–C(11)	1.75(2)	Au···Au	6.83
P(1)–Au(1)–Cl(1)	178.8(2)	C(11)–P(1)–Au(1)	114.0(9)
C(11)–P(1)–C(1)	105.3(11)	C(1)–P(1)–Au(1)	115.5(7)
C(11)–P(1)–C(5)	105.1(10)	C(5)–P(1)–Au(1)	112.6(8)
C(1)–P(1)–C(5)	103.2(10)		

Table 3. Bond Lengths (Å) and Angles (deg) for $3(\text{ClO}_4) \cdot 2\text{CH}_3\text{CN}$

Au(1)···Au(1A)	2.8261(11)	P(1)–C(5)	1.802(14)
Au(1)–P(1)	2.238(3)	P(1)–C(11)	1.812(15)
Au(1)–N(1)	2.090(11)	P(1)–C(1)	1.835(14)
P(1)–Au(1)–N(1)	178.0(4)	C(5)–P(1)–C(11)	109.7(7)
N(1)–Au(1)–Au(1A)	88.1(4)	C(5)–P(1)–C(1)	105.7(6)
P(1)–Au(1)–Au(1A)	90.89(11)	C(11)–P(1)–C(1)	107.8(7)

(1)–Cl(1) separations of 2.227(6) and 2.293(7) Å, respectively. The Au(1)–P(1)–C(1), Au(1)–P(1)–C(5), and Au(1)–P(1)–C(11) angles are expanded from the ideal tetrahedral angles (109.5°) to 115.5(7), 112.6(8), and 114.0(9)°, respectively.

Colorless crystals of both $3(\text{ClO}_4)$ and $3(\text{BF}_4)$ are obtained in two ways. The first method is capable of producing either the “orange” or “blue” form while the second method yields exclusively the “blue” form. X-ray-quality crystals can be grown by slow diffusion of diethyl ether into the acetonitrile filtrate of the initial reaction mixture at -5°C . The thermal ellipsoid plot of the cationic portion of the identical structures of $3(\text{ClO}_4)$ and $3(\text{BF}_4)$ is presented in Figure 5 with selected bond distances and angles in Tables 3 and 4. The crystals obtained visibly luminesce orange, and only a few are suitable for X-ray analysis. These crystals can be recrystallized from acetonitrile/diethyl ether at either -5°C or room temperature. This procedure nearly quantitatively yields crystals that visibly luminesce blue, and the bulk of the crystals are X-ray quality. The four species, $3(\text{ClO}_4)$ (“orange” and “blue”) and $3(\text{BF}_4)$ (“orange” and “blue”), all

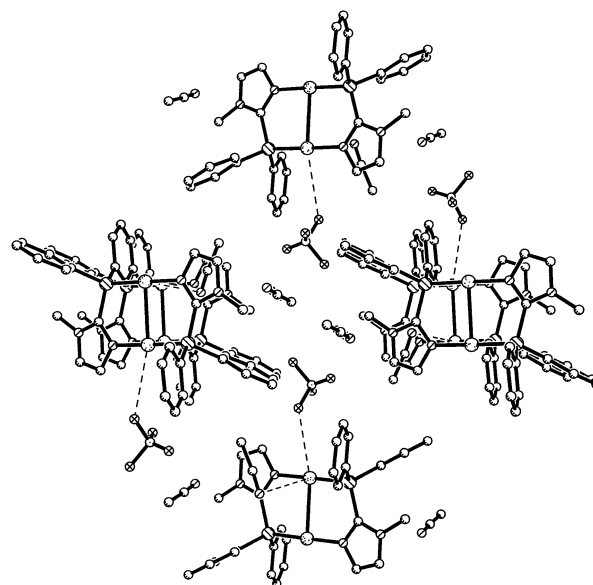


Figure 6. Packing diagram of $3(\text{ClO}_4)_2$ arbitrarily oriented to emphasize the perchlorate–Au(I) contacts within the lattice.

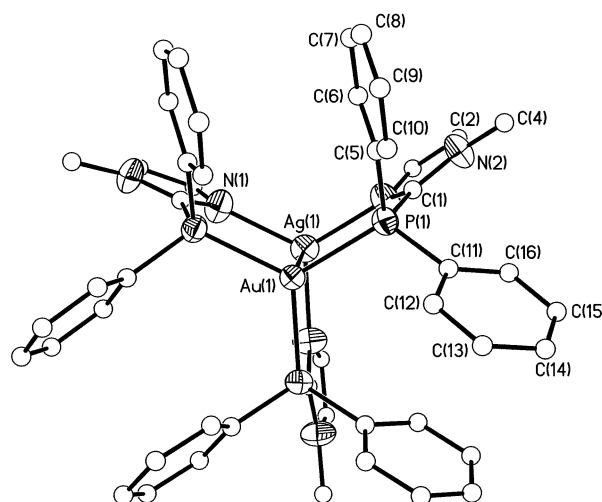


Figure 7. X-ray structural drawing of the cationic portion of **4** emphasizing the 3-fold symmetry. Hydrogen atoms have been removed and carbon atoms drawn as open circles for clarity. Only the crystallographically unique portion is labeled.

crystallize in the monoclinic $P2_1/n$ space group with the Au–Au vector residing on a crystallographic inversion center, making only half of the complex crystallographically unique. The two Au atoms are bridged by two dpim ligands in a head to tail fashion, with each Au coordinated to the phosphorus atom of one ligand and the imidazole nitrogen of the second ligand. The N–Au–P angles are nearly linear and range from 177.9(3) to 178.0(4)°. The Au–N and Au–P separations range from 2.083(9) to 2.090(11) Å and 2.235(3) to 2.238(3) Å, respectively, while the aurophilic Au–Au separations are short and range from 2.8174(10) to 2.8261(11) Å. The anions and solvent molecules show a slight attraction toward the Au atoms with one solvent and two anion contacts per Au dimer. As shown in Figure 6, the perchlorate anion weakly interacts with the Au center with the shortest Au–O separation being 3.22(7) Å.

Table 4. Bond Lengths (Å) and Angles (deg) for **3**(BF₄)·2CH₃CN

Au(1)···Au(1A)	2.8174(10)	P(1)–C(5)	1.814(12)
Au(1)–P(1)	2.235(3)	P(1)–C(11)	1.808(12)
Au(1)–N(1)	2.083(9)	P(1)–C(1)	1.812(11)
P(1)–Au(1)–N(1)	177.9(3)	C(5)–P(1)–C(11)	108.8(5)
N(1)–Au(1)–Au(1A)	88.3(3)	C(5)–P(1)–C(1)	106.0(6)
P(1)–Au(1)–Au(1A)	90.91(9)	C(11)–P(1)–C(1)	107.2(6)

Table 5. Bond Lengths (Å) and Angles (deg) for **4**

Au(1)···Ag(1)	2.8635(15)	P(1)–C(5)	1.809(10)
Au(1)–P(1)	2.374(2)	P(1)–C(1)	1.821(10)
Ag(1)–N(1)	2.236(8)	P(1)–C(11)	1.812(7)
P(1)–Au(1)–P(1A)	119.979(3)	C(5)–P(1)–C(11)	105.8(4)
N(1)–Ag(1)–Au(1)	86.3(2)	C(5)–P(1)–C(1)	103.7(5)
P(1)–Au(1)–Ag(1)	90.84(7)	C(11)–P(1)–C(1)	108.6(4)

Colorless, X-ray-quality crystals of **4** were obtained by slow diffusion of diethyl ether into a saturated acetonitrile solution at room temperature. The structural drawing of **4** is represented in Figure 7, with selected bond distances and angles in Table 5. The colorless complex crystallizes in the cubic space group *Pa*–3, with the Au–Ag bond lying on a 3-fold rotational axis, making only 1/3 of the molecule unique. The Au–Ag separation is 2.8635(15) Å. Due to the high crystallographic symmetry of the molecule, the three Au–P distances are equivalent (2.374(2) Å) as are the three Ag–N bond distances (2.236(8) Å). The P–Au–P angles are nearly ideally trigonal planar at 119.979(3)°, as are the N–Ag–N angles of 119.59(5)°. The P–Au–Ag and N–Ag–Au bond angles are 90.84(7) and 86.3(2)°, respectively.

Discussion

The dpim ligand allows the facile formation of gold(I) and silver(I) homo- and heterobimetallic complexes possessing interesting structural and photophysical properties. Complex **1** is a discrete dimer with an Ag–Ag separation of 2.9932(9) Å. This separation is shorter than that of [Ag₂(dppy)₂](NO₃)₂ (3.146 Å),²⁵ where dppy = bis(diphenylphosphino)pyridine. The two complexes have very similar metal to ligand (Ag–P and Ag–N) bond distances of 2.3807(14) and 2.198(4) Å in **1** and 2.378(2) and 2.234(6) Å in the dppy complex, respectively.^{22,25} While **1** and the dppy complex are structurally similar, they are strikingly different than the [Ag₂(dpim)₂](NO₃)₂ complex recently reported by Nishikawa and co-workers.²² [Ag₂(dpim)₂](NO₃)₂ consists of Ag–Ag dimers connected by Ag–ONO₂ interactions to form a polymeric chain. Although the Ag–P and Ag–N separations (2.391(3) and 2.214(9) Å)²² are similar to **1**, the Ag–Ag separation (2.918(3) Å)²² is slightly shorter than that found in **1**. The ³¹P{¹H} NMR spectrum of **1** shows a broad multiplet at –4.9 ppm, consistent with the dppy and nitrate polymer complexes.^{22,25} There were no luminescent properties reported for the dppy or nitrate polymer complex; therefore, no comparisons can be made. However, complexes containing Ag–Ag interactions are known to be luminescent.

For example, the phosphine-bridged [Ag₃(dppn)₃]³⁺, where dppn is 2,9-bis(diphenylphosphino)-1,8-naphthyridine, that contains an Ag–Ag separation of 3.145(2) Å^{20a} is intensely luminescent with a broad emission band at 550 nm whereas **1** emits at 442 nm (λ_{exi} = 335 nm).²⁶ Additionally, this species also contains a solvent molecule (DMSO) coordinated to the Ag similar to the acetonitrile bound to Ag in **1**.^{20a}

The monomeric gold(I) complex (**2**) can be considered analogous to the ((BzIm)Ph₂P)AuCl complex reported by Burini and co-workers.¹² The Au–P and Au–Cl bond lengths of 2.227(6) and 2.293(7) Å respectively, are not significantly different from the (BzIm)Ph₂P derivative (2.303(4) and 2.239(3) Å).¹² However, there are two significant differences that may be considered the results of crystal packing forces. The P–Au–Cl bond angle of **1** (178.8(2)°) is much closer to the value reported for Ph₃PAuCl (179.68°)²⁷ than to that of (BzIm)Ph₂PAuCl (175.1(3)°).¹² The aurophilic Au–Au intermolecular separations in (BzIm)Ph₂PAuCl are 3.03(2) Å,¹² whereas compound **2** exhibits no intermolecular Au–Au interactions, with the closest separation being 6.83 Å. Complex **2** exhibits an intense solid-state emission at 493 nm (λ_{ex} = 335 nm) at room temperature. This closely relates to the solid-state emission of Ph₃PAuCl (λ_{max} = 491 nm, λ_{ex} = 330 nm),¹¹ also at room temperature, suggesting that the emission is likely to be intraligand (π–π*) in nature.

The dimeric gold(I) complex (**3**) has an Au–Au separation of ~2.82 Å for both the perchlorate and tetrafluoroborate salts. This separation is consistent with other gold(I) dimers, including [dmpp₂Au₂]²⁺ (2.776 Å),¹⁴ [(dppm)₂Au₂]²⁺ (2.982 Å),¹¹ and various [(dcpm)₂Au₂]²⁺ dimers (2.9063(9)–3.0132(6) Å).⁹ The closest anion–Au contacts in **3**(ClO₄) are ~3.22 Å, which agree with those seen in [Au₂(dcpm)₂](ClO₄)₂ (3.36(2) Å).^{9a}

The solution-state absorption and emission properties of complex **3** are independent of anion. The electronic absorption spectrum of **3** in acetonitrile (6 × 10^{–6} M) shows only absorptions similar to that of the free dpim ligand. This is in sharp contrast to both the [Au₂(dppm)₂](BF₄)₂¹¹ and [Au₂(dcpm)₂](ClO₄)₂^{9a} dimers, which display intense absorptions at 293 and 277 nm, respectively. These absorptions have been assigned as dσ* → pσ transitions.^{9,11} For [Au₂(dppm)₂](BF₄)₂, this absorption closely resembles the excitation spectrum in solution, giving rise to an emission at 593 nm (λ_{ex} = 293 nm).¹¹ Complex **3** exhibits a much higher energy emission at 360 nm (λ_{ex} = 290 nm) in acetonitrile at room temperature. The differences in solution electronic absorption and emission can be explained by considering the different donor abilities of dppm versus dpim. Assuming dpim to be a weaker donor to gold(I) than dppm, the Au–Au interactions would be weakened such that the dσ* → pσ transition is much higher in energy for **3** versus [Au₂(dppm)₂](BF₄)₂. The absorption band associated with this transition will then overlap with the π–π* transitions of the ligand. The solution state emission of **3** shows two bands, similar to the ligand

(23) Pangborn, A. B.; Giardello, M. A.; Grubbs, R. H.; Rosen, R. K.; Timmer, F. J. *Organometallics* **1996**, *15*, 1518–1520.

(24) Uson, R.; Laguna, A.; Laguna, M. *Inorg. Synth.* **1989**, *26*, 85–91.

(25) Liu, H. F.; Liu, W.; Zhang, P.; Huang, M. S.; Zhen, L. X. *Xiamen Daxue Xuebao Ziran Kexueban* **1992**, *31*, 57–60.

(26) Uang, R.-H.; Chan, C.-K.; Peng, S.-M.; Che, C.-M. *J. Chem. Soc., Chem. Commun.* **1994**, 2561–2562.

(27) Baenziger, N. C.; Bennett, W. E.; Soboroff, D. M. *Acta Crystallogr. B* **1976**, *32*, 962–963.

in solution. This suggests that in the absence of the solid-state anion–cation exciplex interactions the intraligand bands predominate the solution spectra.

Perhaps the most striking feature of this work is the unusual blue–orange emissions observed for **3**, independent of anion ($\text{BF}_4^-/\text{ClO}_4^-$) or solvents of crystallization. The “orange” and “blue” forms have identical crystal structures, suggesting that the origin of the difference in luminescent properties lies in a minor impurity not visible by X-ray diffraction rather than a conformational change. An undetectable impurity within the crystal structure is possible if there is a small amount of impurity that resides in the same position as an anion or solvent molecule. This impurity could include a minor amount of acid (from ligand purification), water (from wet solvents), or Cl^- (from incomplete halide abstraction), all of which were explored. Solutions of **3** (“blue” form) in acetonitrile were intentionally doped with varying concentrations of acid and water, and crystals were grown from each solution. Each attempt produced only “blue” crystals. Likewise, addition of small amounts of triethylamine produced similar results.

The increase of emission intensity upon grinding is not well-understood, but it does not appear to be related to a phase change because powders formed by the evaporation of solutions of **3** are equally emissive. Recently, Eisenberg and Lee²⁸ reported the reversible luminescence tribromism from a structurally related gold(I) thiouracilate dimer whose unique emissive properties can be related to two different structural motifs interconverted by protonation of the uracilate ligand. Likewise, complex **3** also possess an imine base within the imidazole framework; however, it appears unresponsive to protonation, suggesting a different mechanism is responsible for its emission. Fackler and co-workers²⁹ reported a similar change in emission intensity upon grinding for their linear one-dimensional chain compound $[(\text{TPA})_2\text{Au}][\text{Au}(\text{CN})_2]$, where TPA is 1,3,5-triaza-7-phosphaadamantine. Single crystals of this material are nonemissive but become strongly photoluminescent after grinding. This property was attributed to the generation of lattice defects near the surface. A similar mechanism may be present in this work. Heating samples of **3** to eject the acetonitrile molecules of solvation could also disrupt the lattice producing similar defects.

Conversion of the “orange” form to the “blue” form undoubtedly involves a different mechanism—most likely the inclusion of an impurity. Treatment of an acetonitrile solution of **3** with a methanolic slurry of potassium chloride followed by evaporation yielded a solid residue that luminesces orange, suggesting that Cl^- is indeed a contaminant of **3** in the “orange” crystals. However, upon dissolution in acetonitrile and crystallization by addition of diethyl ether only the monomeric complex **2** is obtained. This is in agreement with the observation that during the recrystallization of the original “orange” form, the purported $[\text{Au}_2(\text{dpim})_2]\text{Cl}_2$ dissociated

into the stable and highly crystalline $\text{Au}(\text{dpim})\text{Cl}$ (**2**). Further, the formation of **2** can be followed by ^{31}P NMR spectroscopy where successive addition of tetrabutylammonium chloride shifts the resonance of **3** toward that of **2**. Attempts to directly synthesize $[\text{Au}_2(\text{dpim})_2]\text{Cl}_2$ independently have only yielded **2**. The red-shifted luminescence of the possible $[\text{Au}_2(\text{dpim})_2]\text{Cl}_2$ versus **3** is consistent with red-shifted luminescence displayed by $[\text{Au}_2(\text{dcpm})_2]\text{I}_2$ versus $[\text{Au}_2(\text{dcpm})_2](\text{BF}_4)_2$ reported by Che, as is the similar emission of either the BF_4^- or ClO_4^- salts.^{9a} Additionally, the relative increase of the low-energy emission band upon concentration of the acetonitrile solution of **3** is consistent with the exciplex mechanism proposed by Che and co-workers.⁹ The relative intensities of these disparate emissions, “blue” powder > “blue” crystal > “orange” crystal, are also in line with the emissive properties of $[\text{Au}_2(\text{dppm})_2](\text{BF}_4)_2$.¹¹

Three-coordinate gold(I) complexes have been shown to exhibit intense luminescent properties.²¹ However, to the best of our knowledge, complex **4** is the first structurally characterized three-coordinate Au–Ag dimer and one of only a handful of Au–Ag heterobimetallic dimers to be structurally characterized.¹⁵ Interestingly, attempts to synthesize $[\text{AuAg}(\text{dpim})_2]^{2+}$ resulted only in the formation of **4**. The hypothetical $[\text{AuAg}(\text{dpim})_2]^{2+}$ was expected to be analogous to $\text{AgAu}(\text{MTP})_2$. However, the reaction resembles that seen by Burini, in the $[\text{Ag}_2(\text{BzIm})\text{Ph}_2\text{P})_3]^{2+}$ complex.¹² The $^{31}\text{P}\{-^1\text{H}\}$ NMR spectrum is insensitive to ligand:Ag:Au ratios (2:2:1 or 3:2:1) with the product consistently exhibiting a single sharp resonance at 17.5 ppm, suggesting that there is no equilibrium present between **4** and $[\text{AuAg}(\text{dpim})_2]^{2+}$.

The Au–Ag separation of 2.8635(15) Å is between that of $\text{AgAu}(\text{MTP})_2$ (2.9124(13) Å)¹⁵ and the $[\text{AuAg}(\text{dppy})_2]^{2+}$ complex (2.820(1) Å).¹⁰ $\text{AgAu}(\text{MTP})_2$ was reported to be luminescent in the solid state at 77 K ($\lambda_{\text{em}} = 420$ nm, $\lambda_{\text{ex}} = 335$ nm).¹⁵ Compound **4** is also luminescent in the solid state at room temperature with an emission at 490 nm ($\lambda_{\text{ex}} = 360$ nm). The emission is surprisingly similar to **3**, as **4** appears yellow to the naked eye while **3** appears blue. However, the emission intensity of **3** is much higher than that of **4**.

Conclusion

The dpim ligand allows the facile formation of gold(I) and silver(I) homo- and heterobimetallic complexes. The complexes exhibit luminescent properties similar to those reported for other various $d^{10}\text{--}d^{10}$ binuclear complexes. dpim also favors a three-coordinate Au(I)–Ag(I) heterobimetallic complex that is unprecedented in the literature.

For the intensely luminescent Au(I)–Au(I) dimer, $3(\text{ClO}_4)_2$, the close proximity of the anion and the high probability of emission dependence upon coordinating versus noncoordinating anions closely resemble the $[\text{Au}_2(\text{dcpm})_2]^{2+}$ complexes reported by Che and co-workers.^{9a} These results appear to support Che’s conclusion that the luminescent behavior of Au(I)–Au(I) dimers arises from exciplex formation with anions or solvent. The unusual orange/blue emission of **3** is likely a result of a Cl^- partially occupying the position where traditionally noncoordinating anions typically reside.

(28) Lee, Y.-A.; Eisenberg, R. *J. Am. Chem. Soc.* **2003**, *125*, 7778–7779.
 (29) Assefa, Z.; Omary, M. A.; McBurnett, B. G.; Mohamed, A. A.; Patterson, H. H.; Staples, R. J.; Fackler, J. P., Jr. *Inorg. Chem.* **2002**, *41*, 6274–6280.

Table 6. Crystallographic Data for 1–4

	1·3CH ₃ CN	2	3(ClO ₄) ₂ ·2CH ₃ CN	3(BF ₄) ₂ ·2CH ₃ CN	4
formula	C ₄₀ H ₄₄ Ag ₂ Cl ₂ O ₈ N ₉ P ₂	C ₁₆ H ₁₅ AuClN ₂ P	C ₃₆ H ₃₆ Au ₂ Cl ₂ O ₈ N ₆ P ₂	C ₃₆ H ₃₆ Au ₂ B ₂ F ₈ N ₆ P ₂	C ₄₈ H ₄₅ AgAuB ₂ F ₈ N ₆ P ₃
fw	559.66	498.69	608.72	632.15	1277.27
a, Å	13.4304(10)	9.8042(13)	9.148(4)	9.071(3)	21.535(2)
b, Å	16.6652(18)	12.3697(17)	18.191(3)	18.202(3)	21.535(2)
c, Å	11.737(2)	13.267(2)	14.1585(19)	14.122(4)	21.535(2)
β, deg	109.693(10)	90	90.867(17)	90.855(16)	90
V, Å ³	2473.4(6)	1608.9(4)	2355.9(11)	2331.4(10)	9987.0(16)
space group	P2 ₁ /c	P2 ₁ 2 ₁ 2 ₁	P2 ₁ /n	P2 ₁ /n	Pa-3
Z	4	4	4	4	8
D _{calc} , g/cm ³	1.503	2.059	1.716	1.801	1.699
cryst size, mm ³	0.24 × 0.50 × 0.40	0.10 × 0.48 × 0.12	0.46 × 0.50 × 0.50	0.42 × 0.66 × 0.42	0.42 × 0.44 × 0.44
μ(Mo Kα), mm ⁻¹	3.673	9.403	3.934	6.424	3.494
λ, Å	0.710 73	0.710 73	0.710 73	0.710 73	0.710 73
temp, K	298(2)	298(2)	298(2)	298(2)	298(2)
transm factors	0.48–0.65	0.16–0.41	0.39–0.46	0.18–0.53	0.28–0.42
R ₁ , wR ₂ (I ≥ 2σ(I))	0.0511, 0.1329	0.0575, 0.1353	0.0611, 0.1541	0.0555, 0.1149	0.0487, 0.1196

Experimental Section

All solvents were purified with a Grubbs apparatus.²³ dpim²² and (tht)AuCl²⁴ were prepared from literature procedures. ¹H chemical shifts are reported relative to TMS, and ³¹P{¹H} chemical shifts are reported relative to 85% H₃-PO₄. Combustion analysis was performed by Desert Analytics, Tucson, AZ. UV–vis spectra were obtained using a Hewlett-Packard 8453 diode array spectrometer (1 cm path-length cells). Emission data were recorded using a Spex Fluoromax steady-state fluorometer.

Preparation of [(dpim)₂Ag₂(CH₃CN)₂](ClO₄)₂, 1. A 50 mL Erlenmeyer flask was charged with 20 mL acetonitrile, a stir bar, 191 mg (0.72 mmol) of 2-(diphenylphosphino)-1-methylimidazole (dpim), and 149 mg (0.72 mmol) of silver perchlorate monohydrate. The solution was stirred at room temperature for 10 min. Solvent was removed via rotary evaporation and the residue triturated with diethyl ether to give colorless crystals. The crystals were collected via vacuum filtration and washed with diethyl ether. Yield: 0.2555 g (75%) ¹H NMR (CD₃CN, 25 °C): δ 7.53 ppm (m), δ 7.14 (s), δ 3.32 ppm (s). ³¹P{¹H} NMR (CD₃CN/CH₃CN, 25 °C): δ -4.9 ppm (m).

Preparation of Au(dpim)Cl, 2. To a stirred solution of 65.4 mg (0.25 mmol) of dpim in acetonitrile (10 mL) was added a 10 mL acetonitrile solution of 78.4 mg (0.25 mmol) of (tht)AuCl. The resulting solution was stirred for 15 min. The volume of solvent was reduced (~10 mL) over mild heat. Colorless crystals of **2** form upon cooling to 0 °C. The crystals were then collected via vacuum filtration and washed with diethyl ether. Yield: 82.8 mg (68%). ¹H NMR (CDCl₃, 25 °C): δ 7.60 ppm (m), δ 7.17 (s), δ 3.91 ppm (s). ³¹P{¹H} NMR (CDCl₃, 25 °C): δ 12.1 ppm (s). Anal. Calcd for C₁₆H₁₅AuClP₂: C, 38.53; H, 3.03; N, 5.62. Found: C, 38.79; H, 3.08; N, 5.65.

Preparation of [(dpim)₂Au₂](ClO₄)₂, 3(ClO₄)₂. A 125 mL Erlenmeyer flask was charged with 40 mL of acetonitrile, a stir bar, 365 mg (1.4 mmol) of 2-(diphenylphosphino)-1-methyl imidazole, and 438 mg (1.4 mmol) of (tht)AuCl. The solution was stirred at room temperature for approximately 10 min. A 20 mL acetonitrile solution of 284 mg (1.4 mmol) of silver perchlorate monohydrate was added dropwise. A white precipitate forms upon addition, and the suspension

was stirred for 5 min. The suspension was filtered through a pad of Celite to remove the precipitate. The colorless filtrate was collected and layered with diethyl ether. Orange luminescing colorless crystals formed from the solution at -5 °C. The crystals were collected via vacuum filtration, and washed with diethyl ether. Yield: 0.6700 g (87%). Blue luminescing crystals are prepared by dissolution of the material in a minimum amount of acetonitrile and precipitation with diethyl ether. ¹H NMR (CD₃CN, 25 °C): δ 7.60 ppm (m), δ 3.32 ppm (s). ³¹P{¹H} NMR (CD₃CN/CH₃CN, 25 °C): δ 19.0 ppm (s). Anal. Calcd for C₃₂H₃₀Au₂-Cl₂O₈P₂N₄: C, 34.15; H, 2.69; N, 4.98. Found: C, 34.15; H, 2.69; N, 4.96.

Preparation of [(dpim)₂Au₂](BF₄)₂, 3(BF₄)₂. The preparation of 3(BF₄)₂ was similar to that of 3(ClO₄)₂ using 54.3 mg (0.20 mmol) of dpim, 65.4 mg (0.20 mmol) of (tht)-AuCl, and 39.8 mg (0.20 mmol) of AgBF₄. Yield: 104 mg (81%).

Preparation of [(dpim)₃AuAg](BF₄)₂, 4. A 50 mL Erlenmeyer flask was charged with 20 mL of acetonitrile, a stir bar, 139 mg (0.52 mmol) of dpim, and 55.9 mg (0.17 mmol) of (tht)AuCl. The solution was stirred at room temperature for approximately 10 min. A 10 mL acetonitrile solution of 72.1 mg (0.35 mmol) of silver tetrafluoroborate was added dropwise. A white precipitate forms upon addition, and the suspension was stirred for 5 min. The suspension was filtered through a pad of Celite. The colorless filtrate was collected, and the solvent removed via rotary evaporation. The oily residue was triturated with diethyl ether to give a colorless microcrystalline solid. The solid was collected via vacuum filtration and washed with diethyl ether. Yield: 0.2157 g (95%).

¹H NMR (CD₃CN, 25 °C): δ 7.50 ppm (m), δ 7.23 ppm (broad s), δ 3.17 ppm (s). ³¹P{¹H} NMR (CD₃CN/CH₃CN, 25 °C): δ 17.5 ppm (s).

X-ray Crystallography. Crystal data for **1–4** are presented in Table 6. Suitable crystals of **1–4** were coated with epoxy cement and mounted on a Siemens P4 diffractometer. Unit cell parameters were determined by least-squares analysis of 44 reflections with 7.36 < 2θ < 25.08° for **1**, 39 reflections with 10.09 < 2θ < 25.00° for **2**, 43 reflections with 9.66 < 2θ < 25.03° for 3(ClO₄)₂, 25 reflections with

10.41 $< 2\theta < 24.98^\circ$ for $3(\text{BF}_4)_2$, and 43 reflections with $4.625 < 2\theta < 25.195^\circ$ for **4**. A total of 5398 reflections were collected in the range of $2.02^\circ < \theta < 25.00^\circ$, yielding 4350 unique reflections ($R_{\text{int}} = 0.027$) for **1**. For **2**, a total of 2955 reflections were collected in the range of $2.25 < \theta < 22.49^\circ$, yielding 2111 unique reflections ($R_{\text{int}} = 0.0898$). For $3(\text{ClO}_4)_2$, a total of 5276 reflections were collected in the range of $2.24 < \theta < 25.00^\circ$, yielding 4108 unique reflections ($R_{\text{int}} = 0.0512$), while a total of 5324 reflections were collected in the range of $2.24 < \theta < 25.00^\circ$, yielding 4152 unique reflections ($R_{\text{int}} = 0.0752$) for $3(\text{BF}_4)_2$. A total of 7753 reflections were collected in the range of $1.89 < \theta < 22.50^\circ$, yielding 2182 unique reflections ($R_{\text{int}} = 0.0745$).

Calculations were performed using the Siemens SHELX-TL version 5.10 system of programs, refining on F^2 . The

structures were solved by direct methods. Common with room-temperature crystal structures the fluorine and oxygen atoms of the BF_4^- and ClO_4^- anions were positionally disordered around the central atoms. Simple models of this disorder produced satisfactory refinement.

Acknowledgment is made to the National Science Foundation (Grant CHE-0091180) and to the donors of the Petroleum Research Fund, administered by the American Chemical Society, for their generous financial support of this research.

Supporting Information Available: Complete X-ray crystallographic data for **1–4** (CIF format). This material is available free of charge via the Internet at <http://pubs.acs.org>.

IC030200M